35th Annual International Conference of the IEEE EMBS
Osaka, Japan, 3 - 7 July, 2013

A High-frequency Transimpedance Amplifier for CMOS Integrated 2D CMUT Array towards 3D Ultrasound Imaging

Xiwei Huang[1, 2], Jia Hao Cheong[2], Hyouk-Kyu Cha[3], Hongbin Yu[2], Minkyu Je[2], and Hao Yu[1*]

***Abstract*—One transimpedance amplifier based CMOS analog front-end (AFE) receiver is integrated with capacitive micromachined ultrasound transducers (CMUTs) towards high frequency 3D ultrasound imaging. Considering device specifications from CMUTs, the TIA is designed to amplify received signals from 17.5MHz to 52.5MHz with center frequency at 35MHz; and is fabricated in Global Foundry 0.18-µm 30-V high-voltage (HV) Bipolar/CMOS/DMOS (BCD) process. The measurement results show that the TIA with power-supply 6V can reach transimpedance gain of 61dBΩ and operating frequency from 17.5MHz to 100MHz. The measured input referred noise is 27.5pA/√Hz. Acoustic pulse-echo testing is conducted to demonstrate the receiving functionality of the designed 3D ultrasound imaging system.**

I. Introduction

Ultrasound imaging is widely utilized in bio-medical imaging diagnosis [1] because it has much less-harmful characteristic to the human body, lower cost, high penetration depth and real-time imaging capability in comparison to other methods such as X-rays, magnetic resonance imaging (MRI) and computed tomography (CT) [2]. Recently, high frequency (>30MHz) and three-dimensional (3D) ultrasound imaging is becoming the next frontier, because higher frequency yields much improved spatial resolution, and 3D imaging provides width, height and depth information that can greatly increase the capability of analyzing images for bio-medical diagnosis [3-4]. The high frequency and 3D ultrasound imaging requires that: i) two-dimensional (2D) transducer array to transmit acoustic waves at different angles; and ii) high bandwidth analog front-end (AFE) receiver to read out the reflected signals [4]. Thanks to the recent development of silicon capacitive micromachined ultrasound transducers (CMUT) [5], the CMOS integrated ultrasound imaging system becomes feasible with high gain wide bandwidth AFE receiver to read out signals when compared to the conventional piezoelectric transducers [6].

In this paper, we present a high frequency transimpedance amplifier (TIA) as the primary component, preamplifier, in the AFE receiver, which is integrated with 2D CMUT array towards high frequency 3D ultrasound imaging. Different from preamplifiers in previous works [2][4] that are mainly targeted for 2D imaging with bandwidth of only 25MHz and 5.1MHz, our design has targeted bandwidth of 52.5MHz.

The remaining part of this paper is organized as follows. In section II, the CMOS integrated CMUT-array based ultrasound receiver is elaborated in details with design specifications. Then in section III, the TIA design implementation is discussed. The simulation and measurement results are presented in section IV with conclusion in section V.

II. CMUT-array based Ultrasound Receiver

A. CMUT Device Modeling

CMUT is basically a transducer that converts ultrasound acoustic waves into electrical signals and vice versa. The CMUT is operated upon electrostatic force. A DC bias voltage V_{Bias} is applied to one of CMUT electrodes, which causes the membrane to deflect towards the substrate; while an AC pulse is imposed on the device, which causes the membrane to vibrate, and emit acoustic power to surrounding medium. When deployed for reception, the incident acoustic wave with pressure causes a change in the device capacitance, which will be detected by the receiving circuit. This variation in capacitance generates an AC current signal by

$$I_{CMUT} = V_{Bias} \frac{\partial(\Delta C)}{\partial t} = \frac{\partial(\Delta Q)}{\partial t} \quad (1)$$

where ΔC is the change in capacitance, and ΔQ is the proportional change in the amount of charge.

In this work, design parameters of our in-house fabricated CMUT element array are summarized in Table 1. The microscope photos of CMUT cells are shown in Fig. 1 (d) and (e). The equivalent circuit model of CMUT calculated from the device parameters is in Fig. 2. The high voltage DC biasing for the CMUT is done through a large external resistor R_B, and a shunt capacitor C_B is added for AC ground for the CMUT as shown in Fig. 4. The design and fabrication details of the CMUT element are beyond the scope of this paper and will not be further discussed.

Table 1. Design Parameters for CMUT.

Parameter		***Values***
CMUT array (elements)		16×16
CMUT cells per element		20×20
CMUT cell geometrical profile	Width	28µm
	Depth	28µm
	Thickness	3µm
	Gap size	0.1µm
CMUT element dimension		600µm×600µm
CMUT excitation voltage (V_{P-P})		20V
Bandwidth		17.5-52.5MHz
Capacitance variation		2.12aF/Pa
Capacitance per element (deflated)		44pF

Resrach supported by the Science and Engineering Research Council of A*STAR (Agency for Science, Technology and Research), Singapore, under SERC grant number: 1021480008.

X. Huang and H. Yu* are with the School of Electrical and Electronic Engineering, Nanyang Technological University, Singapore 639798 (phone: 65+6790 4509; fax: 65+6793 3318; e-mail: haoyu@ntu.edu.sg).

X. Huang, J. H. Cheong, H. Yu and M. Je are with Institute of Microelectronics, A*STAR (Agency for Science, Technology and Research), Singapore 117685.

H.-K. Cha was with Institute of Microelectronics. He is now with the Dept. of Electrical Engineering and Info. Tech., Seoul National University of Science and Technology, Seoul, Korea 139743.

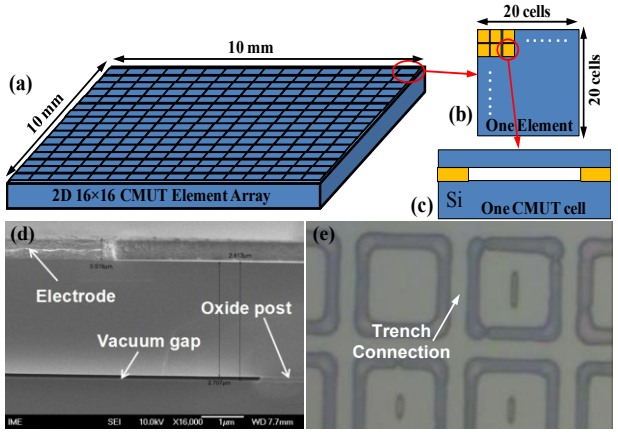

Figure 1. (a) Diagram of CMUT array, (b) one CMUT element, (c) one CMUT cell, (d) cross-section view of CMUT cell, (e) top view of CMUT cells.

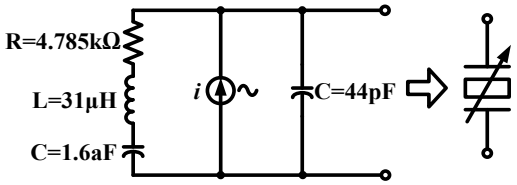

Figure 2. Equivalent simulation model for CMUT.

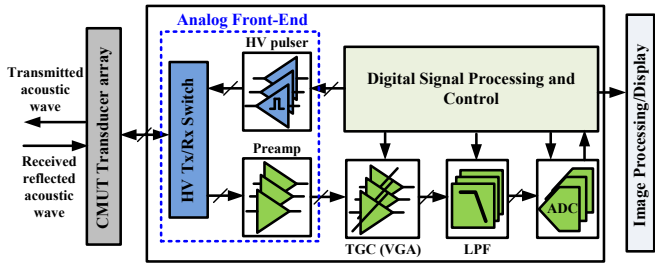

Figure 3. System diagram of ultrasound imaging system with AFE recevier to integrate with CMUT.

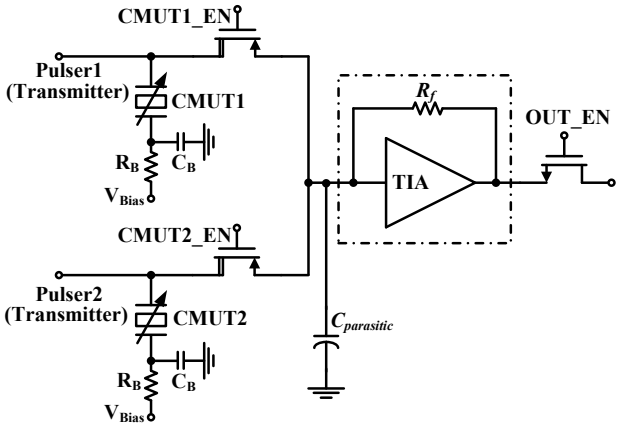

Figure 4. Schematic for one CMOS analog front-end cell of receiver with integrated CMUT.

B. *AFE Receiver*

In one typical ultrasound imaging system, the AFE receiver consists of a HV pulser, a TX/RX protection switch, and a readout preamplifier (*i.e.* TIA in our system) as shown in Fig. 3. Following the preamplifier, the receiving path also includes Time-Gain Compensation (TGC), Low-Pass Filter (LPF) and Analog-to-Digital Convertor (ADC), and signal processing to obtain the final ultrasound image.

The AFE receiver schematic for one readout channel is shown in Fig. 4. As the specified layout area per CMUT element is 600μm×600μm, considering the bonding area constraint, one preamplifier is shared by two AFE channels. An additional parasitic capacitance of 1pF is included in simulation between the TIA input and ground considering the bonding for the CMUT element and the TIA [4]. Between the pulser and the preamplifier, a HV protection switch using HV double-diffused lateral MOS (DMOS) transistor is placed in order to isolate the preamplifier circuit to avoid possible breakdown in the transmit mode. It also helps select the individual CMUT element during the echo receiving mode. The outputs of preamplifiers are controlled by output enable switches.

III. TIA Circuit Design and Implementation

A. *TIA Design Specifications*

As the preamplifier is used to read out the received signal from CMUT, its specifications are calculated from the CMUT design parameters and system dynamic range requirement [7]. The preamplifier bandwidth needs to cover 100% fractional bandwidth of the CMUT, *i.e.* 52.5MHz, a high frequency in ultrasound imaging application. The gain of the receiver front-end preamplifier is specified so that the output of the preamplifier is to produce a maximum of $1V_{P\text{-}P}$ voltage to the following block. Using equation (1) for this case, the gain of the preamplifier is 61.18dBΩ, calculated from the maximum displacement current value at maximum acoustic pressure. As the input signal to the preamplifier is a current signal, the input referred current noise is determined by the case when the minimum acoustic-wave pressure echo signal is received. The required input referred current noise of the preamplifier is calculated to be less than 1.15μArms integrated over 35MHz of bandwidth. The output load of preamplifier is 3.2pF//0.31MΩ input impedance of the TGC on PCB.

B. *TIA Design and Analysis*

Acoording to the system design specification, a resistive feedback TIA was selected for low-noise detection, which has ease of biasing and capability to reach high bandwidth [7-8]. The core schematic for TIA is shown in Fig. 5. The TIA is composed of a single-ended amplifier and a feedback resistor R_f. The single-ended amplifier consists of a common-source amplifier followed by an N-type source follower. The TIA acts as a current-to-voltage converter, which has a low input impedance, making it well suited for high-impedance sources and hence maximizing the received input current. The input stage of TIA is the CMUT. During the design simulation, the CMUT equivalent circuit in Fig. 3 was used.

To maximize the input current, the input impedance R_{IN} must be minimized, with $R_{IN} = R_f/(A+1)$, where A is the open-loop gain of the TIA. The value of the feedback resistor R_f and the size of the main input transistor MN1 is critical in deciding the gain, bandwidth, and the noise performance. The close-loop gain of the TIA is set by the feedback resistance R_f of 1.15KΩ, which is translated to a transimpedance gain of 61.18dBΩ.

Moreover, the -3dB bandwidth of TIA is dominated by the capacitance in the large CMUT at the input of TIA by

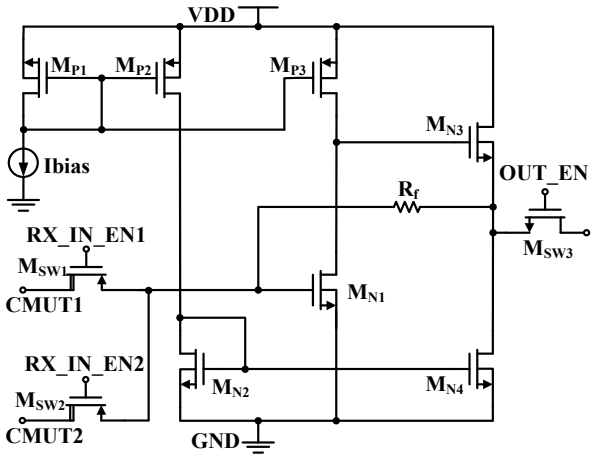

Figure 5. Resistive feedback TIA schematic.

$$\omega_{TIA,-3dB} = \frac{1}{R_{IN}\left(C_{CMUT} + C_{parasitic}\right)} \quad (2)$$

where $C_{parasitic}$ is the parasitic capacitance in parallel with the feedback resistor. Note that the primary noise sources of the TIA are from the common source amplifier and the feedback transistor. With the dominant pole at the input and additional poles at the drain nodes of the transistors MN1 and MP3 and at the output, the phase margin in the open-loop configuration is simulated to be over 55° with a load of 3.2pF//0.31MΩ representing the input impedance of the following TGC.

In addition, the input referred noise current of the TIA can be represented as

$$\overline{i_{N\_in\_total}^2} = \overline{i_{N\_amp}^2} + \overline{i_{R_f}^2} + \overline{v_{N\_amp}^2} \times \left(\frac{1}{R_{in\_amp}} + \omega C_{in} + \frac{1}{R_f}\right)^2 \quad (3)$$

where $\overline{i_{N\_amp}^2}$ and $\overline{v_{N\_amp}^2}$ are the input referred current and voltage noise of the core amplifier, $\overline{i_{R_f}^2}$ is the noise of the feedback resistor, R_{in_amp} is the input resistance of the core amplifier, and C_{in} is the total input capacitance including the CMUT capacitance and the input parasitic capacitance. Note that $\overline{i_{N\_amp}^2}$, $\overline{v_{N\_amp}^2}$ and $\overline{i_{R_f}^2}$ are determined by

$$\overline{i_{N\_amp}^2} \approx (\omega C_{in})^2 \frac{4kT\gamma}{g_{m1}}, \overline{v_{N\_amp}^2} \approx \frac{4kT\gamma}{g_{m1}}, \overline{i_{R_f}^2} = \frac{4kT}{R_f}. \quad (4)$$

As such, the transconductance g_{m1} of MN1 and the value of R_f must be maximized to suppress the noise while considering the bandwidth requirement.

IV. Measurement Results

The TIA was fabricated using Global Foundry 0.18-µm Bipolar/CMOS/DMOS (BCD) process, which can support up to 30V. Deep N-well is also used for the TIA transistors to reduce the noise from the pulser. The die photo of our TIA testing chip is shown in Fig. 6 with the area of 400µm×250µm. A unity gain analog buffer is included on chip for external load driving. The simulated bandwith of the buffer can cover 280MHz, much larger than the TIA bandwidth to prevent

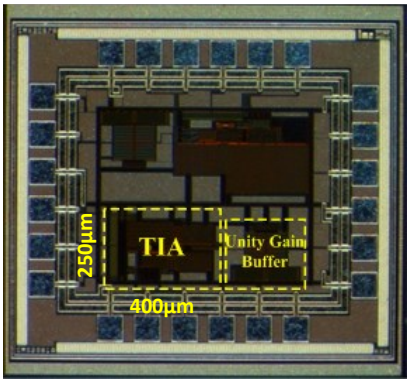

Figure 6. TIA testing chip photo.

impact to TIA during the testing. A QFN24 is used as the die package for measurements on PCB.

The TIA works under a power supply of 6V and 80µA input bias current. The measured total current consumption is 13mA. Due to the large input capacitance from CMUT, sufficient amount of current has been used to meet the bandwidth requirement. During the gain and bandwidth testing, an off-chip resistor was connected in series at the input of the TIA to generate input current. The measured and simulated transimpedance gain-bandwidth is shown in Fig. 7. The operational frequency of the designed TIA can cover up to 100MHz with 61dBΩ transimpedance gain. The gain peaking is due to the introduced parasitic feed-back capacitance that influences the high-frequency open-loop gain of the TIA.

The post-layout simulated input referred current noise at typical operating conditions is 16.8pA/√Hz at 35MHz shown in Fig. 8, which corresponds to a 0.09µArms integrated over 35MHz bandwidth. For measurement, the offline calculated input noise current density from the output noise voltage density is plotted in Fig. 9. As such, the measured input

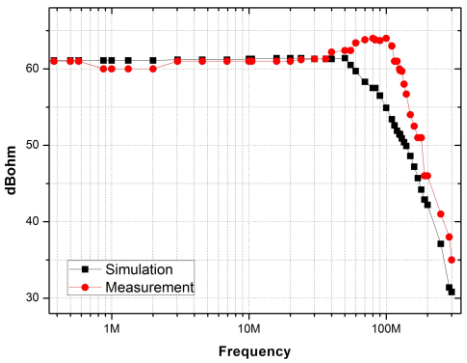

Figure 7. TIA gain and bandwidth simulation vs. measurement results.

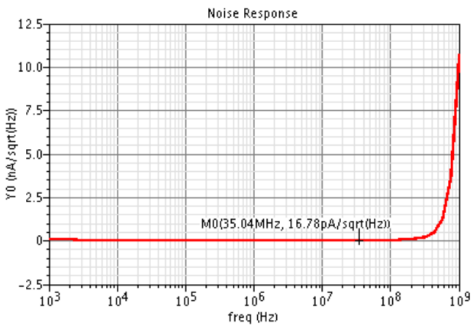

Figure 8. TIA input referred noise simulation results.

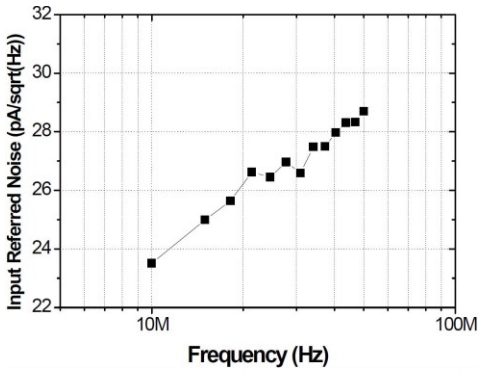

Figure 9. TIA input referred noise measurement results

Table 2. Simulation and measurement results of TIA.

Parameters	*Simulation*	*Measurement*
Transimpedance Gain	61.18dBΩ	61dBΩ
-3dB Bandwidth	75MHz	100MHz
Input Referred Noise	16.8pA/√Hz	27.5pA/√Hz

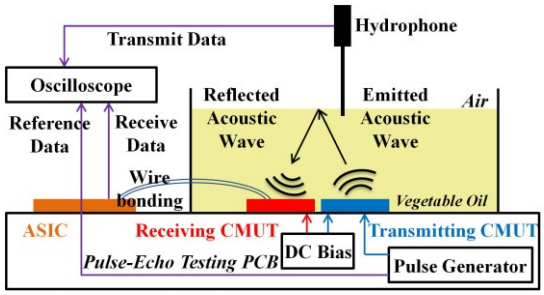

Figure 10. Pulse-echo response measurement setup.

referred noise of the circuit is observed as 27.5pA/√Hz.

Moreover, the acoustic pulse-echo testing was carried out with the AFE IC with CMUT elements. As the testing setup shown in Fig. 10, the devices were mounted on the same PCB and immersed in the vegetable oil contained in a barrel to mimic the underwater environment. We chose one CMUT element from the CMUT array for transmitting and provided it with 20V DC bias voltage. It generated the acoustic wave due to the triggering pulse from the external pulse generator. A hydrophone was immersed into the oil to measure the acoustic pressure as a reference to the TIA output voltage signal. Then the TIA would receive the echo signals resulting from the reflection at the oil-air layer interface. The delay of the received echo can show the pulse-echo distance, which is the depth of the oil inside the barrel. Thus, longer distance between the transmitting CMUT and the oil-air surface results in an increased echo delay. As shown in Fig. 11 (a) for the pulse-echo result, the in-house designed CMUT successfully generated a 6mV acoustic pulse with the triggering from external pulser. Moreover, from Fig. 11 (b), the peak-to-peak voltage of our first echo signal was about 7mV, which also successfully demonstrated the functionality of the developed TIA of the analog-front-end receiver.

V. Conclusion

A CMOS analog front-end (AFE) receiver integrated with CMUT array is demonstrated in this paper for high frequency 3D ultrasound imaging. The AFE receiver has been fabricated using 0.18-μm BCD process. The primary component is a transimpedance amplifier (TIA) that achieves 61dBΩ gain

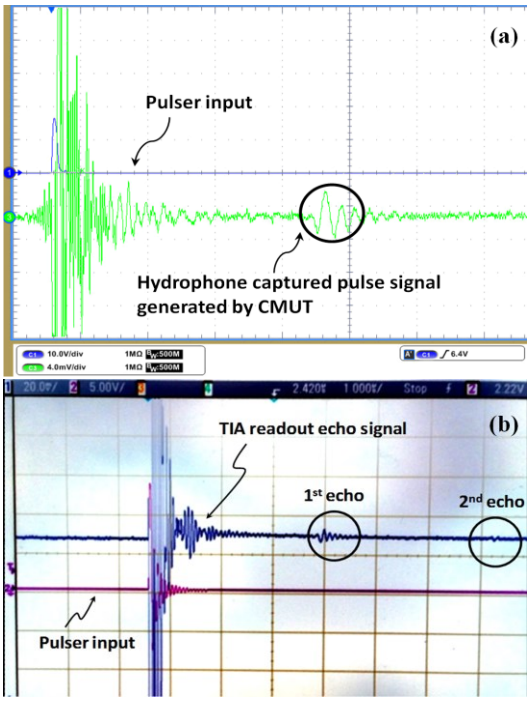

Figure 11. Pulse-echo results (a) CMUT transmitted acoustic pulse signal captured by hydrophone; (b) TIA received echo signals from CMUT.

with 17.5MHz to 100MHz bandwidth, and low input referred noise of 27.5pA/√Hz. The TIA was successfully integrated with CMUT and the functionality of the receiver has been demonstrated with a pulse-echo acoustic testing. Our future work is to demonstrate the whole 3D ultrasound imaging system with digital image processing.

References

[1] P. Levesque and M. Sawan, "Novel low-power ultrasound digital preprocessing architecture for wireless display," *IEEE Trans. Ultrason. Ferroelectr. Freq. Control*, vol. 57, no. 3, pp. 757-767, Mar. 2010.

[2] I. O. Wygant, *et. al.*, "An integrated circuit with transmit beamforming flip-chip bonded to a 2-D CMUT array for 3-D ultrasound imaging," *IEEE Trans. Ultrason. Ferroelectr. Freq. Control*, vol. 56, no. 10, pp. 2145-2156, Oct. 2009.

[3] K. K. Shung, J. Cannata, Q. Zhou, and J. Lee, "High frequency ultrasound: A new frontier for ultrasound," Int. Conf. of the IEEE Engineering in Medicine and Biology Society (EMBC), pp. 1953-1955, 2009.

[4] I. O. Wygant, *et. al.*, "Integration of 2D CMUT arrays with front-end electronics for volumetric ultrasound imaging," *IEEE Trans. Ultrason. Ferroelectr. Freq. Control*, vol. 55, no.2 pp. 327-342, Feb. 2008.

[5] I. Ladabaum, X. Jin, H. T. Soh, A. Atalar, and B. T. Khuri-Yakub, "Surface micromachined capacitive ultrasonic transducers," *IEEE Trans. Ultrason. Ferroelectr. Freq. Control*, vol. 45, no. 3, pp. 678–690, May 1998.

[6] T. R. Gururaja, "Piezoelectric transducers for medical ultrasonic imaging," IEEE Int. Symp. on Applications of Ferroelectrics (ISAF), pp. 259-265, 1992.

[7] I. Kim, *et. al.*, "CMOS Ultrasound Transceiver Chip for High-Resolution Ultrasonic Imaging Systems," *IEEE Trans. Biomed. Circuits Syst.*, vol. 3, no. 5, pp. 293-303, Oct. 2009.

[8] G. Gurun, P. Hasler, and F. L. Degertekin, "Front-end receiver electronics for high-frequency monolithic CMUT-on-CMOS imaging arrays," *IEEE Trans. Ultrason. Ferroelectr. Freq. Control*, vol. 58, no. 8, pp. 1658–1668, Aug. 2011.

[9] L. R. Cenkeramaddi, A. Bozkurt, F. Y. Yamaner, and T. Ytterdal, "A low noise capacitive feedback analog front-end for CMUTs in intra vascular ultrasound imaging," IEEE Ultrason. Symp. (IUS), pp. 2143-2146, 2007.